Review



# [18F]FDG Revisited: A New Perspective on the Temporal Dynamics of Brain Glucose Metabolism

Andreas Hahn *, Pia Falb, Matej Murgas, Sebastian Klug, Murray Reed, Godber Godbersen, Magdalena Ponce de Leon, Christian Milz, Marcus Hacker, Dan Rujescu, Rupert Lanzenberger *

Posted Date: 12 February 2025

doi: 10.20944/preprints202502.0892.v1

Keywords: brain metabolism; functional PET; blood-brain barrier; blood flow; kinetic modeling

*Review*

# [18F]FDG Revisited: A New Perspective on the Temporal Dynamics of Brain Glucose Metabolism

**Andreas Hahn [1,2,*], Pia Falb [1,2], Matej Murgaš [1,2], Sebastian Klug [1,2], Murray B. Reed [1,2], Godber M. Godbersen [1,2], Magdalena Ponce de León [1,2], Christian Milz [1,2], Marcus Hacker [3], Dan Rujescu [1,2] and Rupert Lanzenberger [1,2,*]**

[1] Department of Psychiatry and Psychotherapy, Medical University of Vienna, Vienna, Austria

[2] Comprehensive Center for Clinical Neurosciences and Mental Health (C3NMH), Medical University of Vienna, Vienna, Austria

[3] Department of Biomedical Imaging and Image-guided Therapy, Division of Nuclear Medicine, Medical University of Vienna, Vienna, Austria

* Correspondence: Andreas Hahn, Assoc.Prof. PD PhD MSc; Email: andreas.hahn@meduniwien.ac.at; ORCID: 0000-0001-9727-7580; Rupert Lanzenberger, Prof. PD MD; Email: rupert.lanzenberger@meduniwien.ac.at; ORCID: 0000-0003-4641-9539; Department of Psychiatry and Psychotherapy, Medical University of Vienna, Austria, Waehringer Guertel 18-20, 1090 Vienna, Austria; **ORCID:** Hahn Andreas https://orcid.org/0000-0001-9727-7580; Falb Pia: https://orcid.org/0000-0003-4817-3499; Murgaš Matej: https://orcid.org/0000-0001-7643-2182; Klug Sebastian: https://orcid.org/0000-0001-8714-6608; Reed Murray B: https://orcid.org/0000-0002-4873-608X; Godbersen Godber M: https://orcid.org/0000-0002-9739-0724; Ponce de Leon Magdalena: https://orcid.org/0000-0002-6230-3010; Milz Christian: https://orcid.org/0000-0002-1347-0744; Hacker Marcus: https://orcid.org/0000-0002-4222-4083; Rujescu Dan: https://orcid.org/0000-0002-1432-313X; Lanzenberger Rupert: https://orcid.org/0000-0003-4641-9539

**Abstract:** [18F]FDG positron emission tomography (PET) is extensively utilized to assess brain glucose metabolism, typically through static images reflecting radiotracer accumulation of up to one hour. In comparison, functional PET (fPET) enables investigation of [18F]FDG dynamics occuring within seconds. However, the physiological mechanisms supporting these rapid changes in metabolism necessitate further attention to allow accurate interpretation of brain function and their clinical implications. This work highlights candidate mechanisms driving [18F]FDG signal changes at high temporal resolution, offering complementary insights to existing interpretations. At rest, metabolic demands are closely matched by glucose supply across the blood-brain barrier (BBB), regulated by glucose transporter 1 (GLUT1). During neuronal activation, both glucose transport and phosphorylation by hexokinase are elevated to meet increased energy requirements. Simulations indicate that rapid [18F]FDG signal increases are primarily driven by BBB transport ($K_1$ and $k_2$ in a two-tissue compartment model), with slower subsequent increases in hexokinase activity ($k_3$). Mechanisms supporting increased BBB transport include elevated glucose concentration gradient towards the brain and changes in GLUT1 intrinsic properties, but only minor effects of blood flow. Conversely, moment-to-moment fluctuations in [18F]FDG, as investigated in molecular connectivity, reflect temporally synchronized supply via the BBB to meet metabolic demands. We emphasize that, particularly during neuronal activation, the strong coupling between BBB transport of glucose and metabolism underpin the [18F]FDG fPET signal. Considering alterations of GLUT1 and subsequent metabolism in numerous brain disorders, stimulation-induced changes of energy demands and moment-to-moment fluctuations of molecular connectivity represent a promising opportunity to investigate the underlying pathophysiological processes.

**Keywords:** brain metabolism; functional PET; blood-brain barrier; blood flow; kinetic modeling

 doi:10.20944/preprints202502.0892.v1



## INTRODUCTION

[$^{18}$F]FDG is the most commonly used radiotracer world-wide for positron emission tomography (PET) [1]. This is due to its high clinical relevance in numerous medical fields [2] and the widespread availability given by the simple synthesis with an isotope half-life that allows transportation and commercial production.

Routine clinical use in brain imaging employs a bolus application, followed by a resting period of about 30-60 min and subsequent scanning for 10-15 min [3]. Although this yields only a static image, the (almost) irreversible radiotracer uptake (i.e., $k_4 = 0$ in a 2-tissue compartment model (2TCM), Figure 1) represents a surrogate for the brain glucose metabolism, usually given by the standard uptake value (SUV) or SUV ratio.

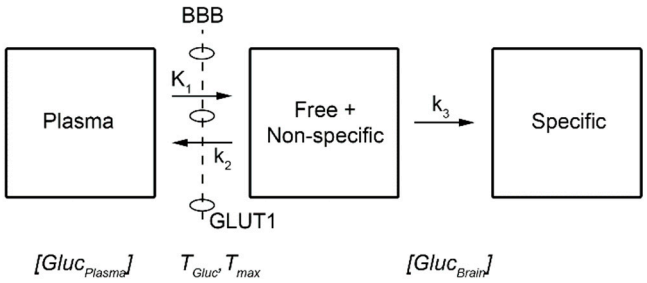


**Figure 1.** *Schematic description of the irreversible two-tissue compartment model, i.e., $k_4 = 0$.* Similar to glucose, the radiotracer [$^{18}$F]FDG crosses the blood-brain barrier (BBB) via facilitated transport by the glucose transporter 1 (GLUT1, 55 kDa), described by rate constants $K_1$ and $k_2$. The uptake mechanism is in contrast to most other radioligands, which cross the BBB via passive diffusion. Within the brain interstitium (free compartment), glucose and [$^{18}$F]FDG are taken up by neurons (GLUT3) and astrocytes (GLUT1, 45 kDA) to be metabolized by hexokinase ($k_3$). The italic variables at the bottom refer to those of Eq. 2, being the concentration of glucose in plasma ([Gluc$_{Plasma}$]) and brain ([Gluc$_{Brain}$]), as well as the maximum ($T_{max}$) and actual transport rate of glucose ($T_{Gluc}$) across the BBB.

While a dynamic PET scan with a bolus application allows for identification of individual rate constants through compartment modeling of the radiotracer kinetics, it will in most cases still yield a static outcome image of the cerebral metabolic rate of glucose (CMRGlu). This can be derived from the influx constant $K_i$, which in turn is a macroparameter obtained from the individual rate constants:

$$K_i = K_1 * k_3 / (k_2 + k_3) \quad (1)$$

These rate constants describe the transport across the blood-brain barrier (BBB, $K_1$ and $k_2$), and the irreversible binding in the cell through the conversion of [$^{18}$F]FDG to [$^{18}$F]FDG-6-phosphate by the enzyme hexokinase ($k_3$), i.e., the first step of glucose metabolism [1] (Figure 1). In most practical applications, SUV(R) and CMRGlu images reflect brain metabolism at resting state, with hexokinase activity being the driving factor at the above mentioned time scale, offering the possibility to identify (non-acute) pathological alterations e.g., caused by epilepsy, tumors, injuries as well as degenerative and psychiatric disorders.

Further advancement of dynamic PET enables the quantification of different cognitive or emotional states within a single PET scan [4–6]. Similar to functional magnetic resonance imaging (fMRI) this is achieved through presentation of e.g., visual paradigms in a block design, thus yielding the term functional PET (fPET). The approach requires administration of radiotracers like [$^{18}$F]FDG as a (bolus +) constant infusion to provide free radioligand throughout the experiment, which is then able to bind according to the current metabolic demands [5,7].

As the temporal resolution for this approach has substantially improved from PET image frames of 1 min [4,5] down to 3 s [8], acute adaptations in glucose metabolism become increasingly relevant. It is therefore essential to determine the assumptions and interpretations that apply to [$^{18}$F]FDG PET

 doi:10.20944/preprints202502.0892.v1



imaging at such a short time scale and to identify the possible neurophysiological mechanisms that underpin rapid changes in metabolic demands. This work aims to highlight major driving factors responsible for fast-acting changes in glucose metabolism and their links to the corresponding [$^{18}$F]FDG signals measured with fPET in vivo. We will specifically focus on aspects applicable to short-term changes, which should be seen in addition to (not instead of) previous knowledge that explained glucose metabolism derived from steady-state kinetics obtained with conventional PET imaging. This work comprises a literature review which supported by with simulations of the irreversible 2TCM (see supplement). We start by briefly re-capitulating the main concepts of brain metabolism from the literature. This knowledge will then be transferred to scenarios of acute stimulation-induced changes in [$^{18}$F]FDG glucose metabolism. Finally, we propose that also moment-to-moment fluctuations in the PET signal at resting state represent meaningful information, but are subject to an even more refined interpretation. In sum, this work provides a neurophysiological account of the rapid dynamics in glucose metabolism elicited through cognitive or emotional processing and at resting-state, which can be imaged with [$^{18}$F]FDG fPET.

## BASAL GLUCOSE METABOLISM IN THE HUMAN BRAIN

The human brain accounts for about 20% of the body's energy demands under resting conditions, with glucose being the primary fuel. Since glucose is only scarcely stored in the brain (except for e.g., glycogen storage in astrocytes, see below), a constant supply from blood is mandatory to maintain brain function [9,10]. Glucose as well as [$^{18}$F]FDG pass the BBB through facilitated transport via the glucose transporter 1 (GLUT1) carrier protein (although at different Michaelis-Menten constants $K_M$) [11–13]. The transport mechanism is required because of the hydrophilic nature of both compounds, which makes [$^{18}$F]FDG different to most other radiotracers which cross the BBB via passive diffusion. Throughout the manuscript, GLUT1 refers to the form with a molecular weight of 55 kDa with highest expression at the BBB (Figure 1), while the 45 kDa form is expressed at astrocytes [11,13].

Glucose transport across the BBB ($T_{Gluc}$) can be described with the Michaelis-Menten equation, taking into account the difference in glucose concentration between blood plasma ([$Gluc_{Plasma}$]) and brain ([$Gluc_{Brain}$], Eq. 2) [14]. It is well known that $T_{Gluc}$ is not the limiting factor under normal resting conditions, but can become so during stimulation (see [14–16] and below). That is, $T_{Gluc}$ has been estimated to be about 30-37% of its maximum value ($T_{max}$ = 1 µmol/g/min, see [9,14,16–18] for assumptions). Rather, the rate limiting aspect at rest seems to be the first step of glucose metabolism, namely conversion by hexokinase [19,20].

$$T_{Gluc} = T_{max}\left(\frac{1}{1+(K_M/[Gluc_{Plasma}])} - \frac{1}{1+(K_M/[Gluc_{Brain}])}\right) \quad (2)$$

The lack of glucose storage in the brain is also in line with the observation that the transport rate of glucose across the BBB closely matches its metabolic rate CMRGlu at about 30 µmol/100g/min [5,9,14,21]. In other words, at resting-state the delivery of glucose just satisfies the actual demands [14,16], which is plausible given the limited storage in the form of glycogen [16,22] and the neurotoxicity of excessive glucose concentrations [23]. These facts in turn imply that acute increases in metabolic demands require an increase in supply across the BBB, i.e. increases in both glucose transport and phosphorylation by hexokinase are required to obtain a feasible increase in energy supply, since neither of these two mechanisms alone is sufficient [16,18].

## STIMULATION-SPECIFIC CHANGES IN [$^{18}$F]FDG

We and others have repeatedly shown that stimulation-induced regional increases in CMRGlu as obtained with [$^{18}$F]FDG in awake humans are stable at about 20-25% from baseline metabolism across various experimental settings [5,14,15,24–26]. It is acknowledged that this is lower than the often referenced 50% [27], but such a large change might be even beyond the maximum calculated transport rate of glucose [15]. Furthermore, recent work has reported increases in regional cerebral

 doi:10.20944/preprints202502.0892.v1



blood flow (CBF) of about 25% [28–31], i.e., a similar range as compared to CMRGlu. Thus, the initially described coupling mechanisms between CMRGlu and CBF [27] still apply.

In line with studies that used other techniques than PET imaging [25,32–34], our recent work has demonstrated that such increases in glucose metabolism may occur almost instantly upon neuronal stimulation [8]. Simulations of the 2TCM (Figure 2) reveal that these initial rapid increases are mainly driven by changes in $K_1$ (and potentially $k_2$), i.e., parameters that characterize BBB transport. On the other hand, irreversible radiotracer binding reflected in $k_3$ occurs at a slower rate, indicating that [$^{18}$F]FDG is truly phosphorylated by hexokinase after transport into the brain. We emphasize that the slower kinetics of $k_3$ apply to [$^{18}$F]FDG that is newly transported across the BBB and the metabolized in response to activation (while glucose metabolism itself is fast). Thus, only a combination of changes in all rate constants matched experimental data. In line, previous work has elegantly shown that only an increase in both glucose transport across the BBB and its phosphorylation by hexokinase yields an increase in overall glucose metabolism [16,18].

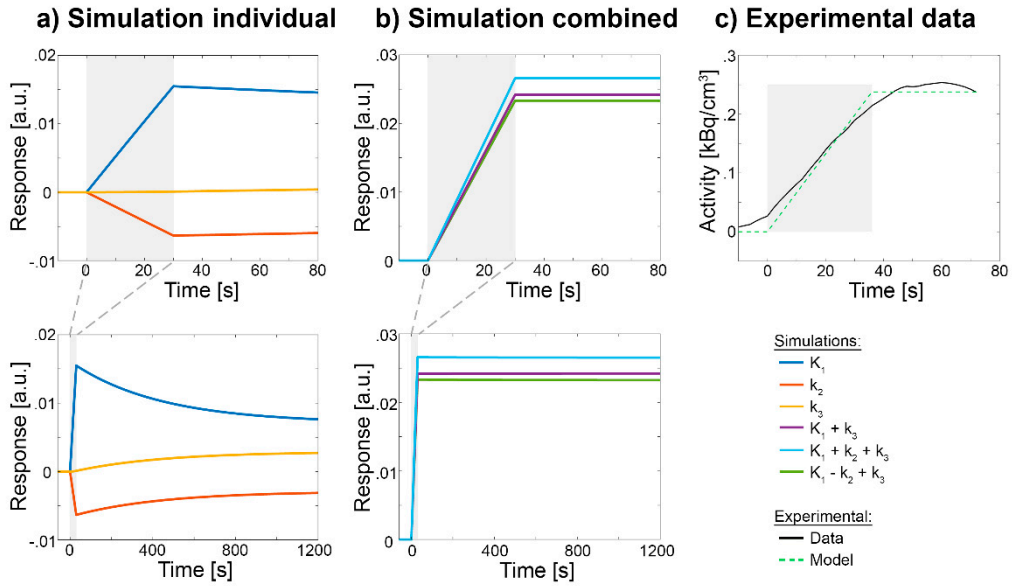


**Figure 2.** *Simulated and experimentally observed changes in the [$^{18}$F]FDG signal upon neuronal activation*. **a)** Simulated increases in individual rate constants indicate that changes in $K_1$ (dark blue) and $k_2$ (red) lead to initially fast, near-linear changes in the fPET signal, whereas changes elicited by $k_3$ (orange) are slower. **b)** Various combinations of changes in $K_1$ and $k_3$ (purple) or $K_1$, $k_2$ and $k_3$ (light blue, green) were simulated to obtain a ramp function, that is typically used to model task-specific changes in glucose metabolism [5]. As the exact contribution of $k_2$ is currently unknown, several cases are provided exemplarily (see supplement for rationale). **c)** Experimentally observed changes in the [$^{18}$F]FDG fPET signal show a rapid increase during the task, which returned to baseline when stimulation ceases [8]. None of the individual rate constants (a) was able to explain the experimentally observed signal changes, but only their combination (b) yielded a comparable effect. Task duration for simulations and experimental data was from 0 to 30 s and from 0 to 36 s, respectively (grey box). See supplementary material for simulation parameters.

This coupling of events may seem trivial, but it is particularly relevant for interpreting the rapid changes observed with fPET. To summarize the essential aspects underpinning the tight coupling of BBB transport and hexokinase activity upon neuronal activation, i) at rest glucose supply just matches the actual demands ($T_{Gluc}$ ~ CMRGlu), ii) there is almost no storage capacity for glucose in the brain, and iii) independent simulations have shown that increases in BBB transport and hexokinase activity are both required to increase the actual metabolism. Again, these results imply that an acute surge in metabolic demands during neuronal activation must consequently also be matched by an increased supply. Previous work has already emphasized that glucose transport across the BBB represents an essential factor at rest [35] and during stimulation [14,15,36]. Of note, even earliest studies assessing

 doi:10.20944/preprints202502.0892.v1



task-specific glucose metabolism imaged BBB transport at least to some extent [37,38]. That is, task performance was carried out during the bolus injection of [$^{18}$F]FDG, with the initial part of the time activity curve (TAC) being mainly determined by $K_1$ and $k_2$.

Although glucose metabolism itself has been studied extensively, the corresponding supply has received relatively little attention, as up until recently, the slower kinetics of $k_3$ where of interest. There are several candidate mechanisms available that may (or may not) explain such an increase in supply (Figure 3). Importantly, with respect to the [$^{18}$F]FDG signal, all of these mechanisms will to some extent affect its transport via the BBB ($K_1$ and $k_2$) and subsequently its metabolism by hexokinase ($k_3$).

Cerebral blood flow (CBF)

The increase in CBF upon neuronal activation is well established and represents the basis of blood-oxygen level dependent (BOLD) fMRI. Among others [39], such changes occur at the level of the capillary bed by decreasing its resistance to and heterogeneity of flow [40–42]. For PET imaging, $K_1$ is often associated with changes in blood flow. This assumption is valid for radiotracers that cross the BBB via passive diffusion and have a high extraction rate. However, as mentioned above glucose and [$^{18}$F]FDG are subject to a facilitated transport mechanism via GLUT1. More importantly, their extraction rate from blood is only 10% [9,14,18,43,44]. This implies that an increase in regional CBF of about 25% by neuronal activation [28–31] would result only in a 2.5% change in BBB transport of glucose, which in turn is only a fraction of the observed CMRGlu change. Experimental work using a hypercapnia challenge also showed that [$^{18}$F]FDG uptake is not influenced by supraphysiological changes in CBF even if higher than 100% [4]. This does not invalidate previous observations showing associations between CBF and CMRGlu. Rather, it suggests that these may be correlated, but only due to their common causal dependency on neuronal activation. Altogether, this suggests that changes in CBF only represent a minor contribution to changes in the [$^{18}$F]FDG signal.

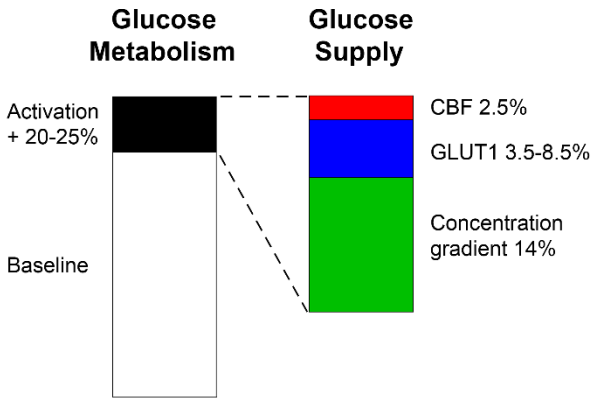


**Figure 3.** Candidate mechanisms contributing to increased glucose metabolism upon neuronal activation via increased glucose supply across the BBB. Based on experimental data [5,14,15,24–26,45,46], a 20-25% increase in regional glucose metabolism from baseline was assumed to be representative, which is distributed as follows. Cerebral blood flow plays only a minor role (2.5%, red), due to the low extraction rate of glucose from blood. The largest part (14%, green) can be explained by an increased glucose concentration gradient from blood to brain. The remaining 3.5-8.5% can be ascribed to alterations of the intrinsic properties in GLUT1, such as conformational changes, unmasking of available molecules and decomposition of GLUT1 clusters into singular molecules. Since an increase in the number of GLUT1 molecules at the BBB occurs only after minutes or hours, this mechanism is not considered to be relevant for rapid changes in glucose metabolism. Notably, BBB changes are here assumed to equally translate into CMRGlu changes, as suggested previously [18]. Even if the assumption may not hold, the ratio between the different mechanisms will probably remain the same.

Glucose concentration gradient

 doi:10.20944/preprints202502.0892.v1



The BBB is not freely permeable for glucose, maintaining a concentration gradient of about [$Gluc_{Plasma}$] = 5 mmol/L in blood plasma vs. [$Gluc_{Brain}$] = 1 mmol/L in brain extracellular space at rest [9,12,14]. During neuronal activation, glucose phosphorylation is accelerated [13], which decreases brain glucose concentration by about 20% [14,25,26,45,46]. Leaving everything else constant in Eq. 2, such an increase in the concentration gradient between blood and brain alone would increase glucose transport across the BBB ($T_{Gluc}$) by 14% [14]. As noted previously, this effect derived from the law of mass action is still insufficient to explain CMRGlu changes in full [17]. Interestingly, the mentioned decrease in [$Gluc_{Brain}$] is very much within the range of regional changes observed with [$^{18}$F]FDG fPET [5,15,24], thereby providing the possible interpretation of fPET signal changes representing just the amount of glucose that is needed to satisfy the increased demands.

Intrinsic properties of GLUT1

Another aspect to modify BBB transport of glucose is given by changes in its permeability, which has also been described as neurobarrier coupling [14]. This is realized by adaptations of the intrinsic properties of GLUT1 upon activation, resulting in an increased $T_{max}$ of Eq. 2 [47,48]. Although rather little is known about the exact changes, potential mechanisms may include conformational changes between occluded and open states [49,50] as well as "unmasking" of already available binding sites [47,51,52]. Interestingly, the increases in $T_{max}$ occurred without relevant changes in $K_m$ [47,53]. Furthermore, GLUT1 appears in clusters, which are dissolved during activation resulting in increased glucose transport [54]. Regarding the temporal scale, one study reported rapid changes in GLUT1 $T_{max}$ within 10 s [55]. However, this concerned the astrocytic GLUT1 transporter (45 kDa), which differs from that of the BBB (55 kDa), so it remains to be investigated whether these effects translate to BBB transport. In any case, slightly delayed increase in the transport is also in line with the above mentioned decrease in brain glucose concentration [25]. Unfortunately, quantitative estimations at short time scales are hardly available so far. One study demonstrated an increase in $T_{max}$ by 30-40%. However, this was obtained after the induction of seizures [56], thus being a supraphysiological stimulus. Considering that the other mechanisms may already account for 16.5% of changes (2.5% CBF + 14% concentration gradient), the remaining amount to reach the commonly observed regional CMRGlu increase of 20-25% would then leave 3.5-8.5% that are attributed to intrinsic changes in GLUT1 (Figure 3).

Number of GLUT1

Finally, a possibility to increase the transport rate of glucose is to increase the number of GLUT1 carrier proteins at the BBB surface. This likely occurs through redistribution of GLUT1 from the intracellular pool (which accounts for up to 40% of total GLUT1) to the membrane surface [11,14]. However, the time-scale at which this occurs has been described to be mostly within the range of minutes to hours [14]. Thus, increased expression of GLUT1 at the BBB may be relevant for subsequent adaptations to sustained neuronal activation, but probably represents a minor factor in the adaptations to meet acute metabolic demands. Also, the above changes in $T_{max}$ may even occur without variations in the number of glucose transporters [47] and mRNA [57].

In sum, these findings suggest that the majority of increases in glucose supply upon neuronal activation are related to an increased concentration gradient towards the brain, followed by changes of the intrinsic properties of GLUT1, whereas increases in blood flow only play a minor role (Figure 3). Thus, the increased supply reflects the fast increase of the [$^{18}$F]FDG signal, which is then followed by its metabolism via hexokinase.

## RESTING-STATE DYNAMICS OF [$^{18}$F]FDG

The assessment of resting-state functional connectivity as derived from BOLD fMRI and EEG [58,59] has made a convincing case that spontaneous fluctuations of brain signals represent biologically meaningful information even in the absence of specific stimulation. This has substantially

 doi:10.20944/preprints202502.0892.v1



changed our understanding about the interaction between brain regions, organized in hierarchical networks each underpinning different physiological functions [60–62].

Although the concept to compute connectivity with PET data was introduced decades ago [63,64], the computation of molecular connectivity has received particular attention in recent years [65–67], due to the ability to obtain reliable high temporal resolution PET data. In analogy to BOLD fMRI functional connectivity, molecular connectivity refers to the correlation of fluctuations of signal time courses between brain regions herein obtained from high-temporal resolution fPET data [65]. It has been shown that the computation of molecular connectivity with [$^{18}$F]FDG data also features structured network organization [66]. However, the actual molecular connectivity pattern markedly differs from that of functional connectivity [66]. This is in line with the above observation that [$^{18}$F]FDG PET is only modestly dependent on CBF. However, the interpretation and the underlying neurophysiological mechanisms of such rapid signal fluctuations in the fPET signal without external stimulation have not been established.

Moment-to-moment fluctuations in [$^{18}$F]FDG

There are various approaches available to compute moment-to-moment fluctuations from [$^{18}$F]FDG fPET data [65,66,68,69], but all with the common aim to remove the cumulative part of the TAC reflecting the irreversible uptake of the radioligand. The most illustrative approach is a bandpass filter, due to the straightforward interpretation in terms of the signals' frequencies. Here, the common frequency range of $0.01 < f < 0.1$ Hz used for BOLD fMRI functional connectivity suggests that the filtered fPET signal is mostly determined by $K_1$ and $k_2$ (i.e., transport across the BBB), rather than $k_3$. That is, the frequency spectrum of simulated changes in each of these rate constants indicates that changes in $k_3$ are simply too slow for a relevant contribution to such signal fluctuations (Figures 2 and 4).

Hence, what is left after the removal of the irreversible uptake are oscillating changes in the signal, both in experimental and simulated data (Figure 4). Considering the ever-changing metabolic demands, it seems plausible that these fluctuations reflect adaptations through a regulatory circuit, aiming to maintain a constant supply of glucose which matches the current consumption, i.e., slight increases and decreases from a steady baseline according to the actual changes in demand. In the hypothetical case that every brain region has equal metabolic demands, this oscillation would be uniform across the entire brain. However, since the brain is never truly at rest [70] and different brain regions are involved in processing distinct stimuli, its metabolic demands also vary across space and time, resulting in a regional variability in this regulatory signal. If two brain regions have equal metabolic demands simultaneously, then also their time courses would be similar and thus correlated, irrespective of their baseline metabolism. These regions can be considered to be metabolically coupled through their common acute changes in metabolic demands [63,64]. Taking into account that these short-term fluctuations in the fPET signal are driven by $K_1$ and $k_2$ (see Figures 2 and 4 and sections above), molecular connectivity would thus refer to temporally coherent metabolic demands, which are in turn matched by corresponding similar changes in BBB transport. Although it might be surprising that $k_3$ does not seem to play a direct role in molecular connectivity, it is of course still relevant. As emphasized throughout this manuscript and within the concept of neurobarrier coupling [14], changes in BBB transport are initially triggered by neuronal activation, subsequently leading to increased glucose consumption and thus increases in $k_3$. In other words, any change in glucose metabolism is just preceded by a proportional change in BBB transport (see above).

 doi:10.20944/preprints202502.0892.v1



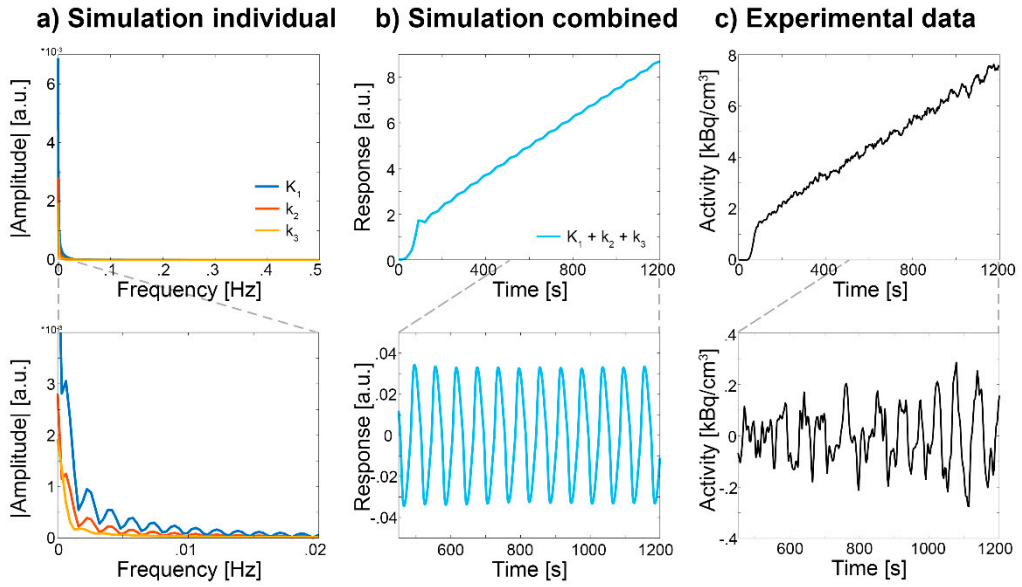


**Figure 4.** *Simulated and experimentally observed changes in the [18F]FDG signal at resting state.* **a)** Frequency spectra of simulated increases in individual rate constants as shown in Figure 2. The excerpt (lower panel) indicates that changes in $K_1$ (dark blue) and to some extent $k_2$ (red) comprise frequency components beyond 0.01 Hz, but not $k_3$ (orange). **b)** Combined changes in $K_1$, $k_2$ and $k_3$ (light blue) exhibit oscillating changes on top of a steady baseline uptake. Rate constants were changed at the same ratio as in Figure 2 (light blue). After applying a bandpass filter these oscillating changes remain (lower panel). Of note, omitting changes in $k_3$ in this simulation showed virtually identical results, indicating that $k_3$ does not contribute to these changes. **c)** Experimentally observed changes in the [18F]FDG fPET signal of a representative subject [89]. Application of a bandpass filter leaves oscillating changes in both the simulated and experimental data (lower panels of b and c), which represent the basis for molecular connectivity.

## LIMITATIONS, OUTLOOK and CONCLUSIONS

Numerous studies with simulations and experimental data demonstrate that stimulation-induced increases in glucose metabolism require BBB transport for subsequent phosphorylation by hexokinase. We emphasize that changes in BBB transport may not be seen independently from hexokinase activity, as neuronal activation triggers both in order to match energy supply and demand, i.e., these mechanisms are strongly coupled. In terms of [18F]FDG PET imaging this implies that several rate constants (especially $K_1$ and $k_3$) are involved in this process. The adaptations supporting neuronal activation are mainly provided by an increased glucose BBB gradient towards the brain and functional changes in the intrinsic properties of GLUT1 molecules, while blood flow plays only a minor role. Conversely, moment-to-moment fluctuations in the [18F]FDG signal used for molecular connectivity seem to reflect the regulation of metabolic supply across the BBB to match the underlying demands.

As a limitation, current models may not yet be sufficient to characterize such rapid changes in glucose metabolism and the corresponding [18F]FDG signal. That is, the Michaelis-Menten equation is valid for the steady-state, an assumption that does not hold for acute changes in neuronal activation. Thus, several variables (e.g., $T_{max}$, $[Gluc_{Brain}]$) become time-variant, which requires a different mathematical solution. For the simulations of the 2TCM, time-dependent rate constants were used, but the changes were only assumed to occur during the task effect at a fixed rate, while temporally varying changes and those beyond the stimulation period are possible. Finally, we acknowledge that other sources apart from glucose may also be used for energy production. For instance, glycogen is stored in astrocytes, but its turnover is slower than that of glucose [18]. Furthermore, recent modelling suggested that glycogenolysis takes place in astrocytes to spare

 doi:10.20944/preprints202502.0892.v1



glucose for neuronal energy metabolism upon activation [15,22]. This model also seemed to explain fluctuations in lactate [71], which may however not represent a major energy source under normal conditions [72].

Nevertheless, the current work outlines potential neurophysiological underpinnings of rapid changes in the [$^{18}$F]FDG signal, thereby once again highlighting the importance of BBB transport to maintain glucose supply during neuronal activation. It is important to note that the described mechanisms do not replace previous assumptions and interpretations of [$^{18}$F]FDG imaging, rather they should be seen as additional considerations specifically relevant for short-term changes.

Future work may build upon this information to investigate if known pathological alterations of brain glucose metabolism can be characterized in more detail. For instance, decreases in GLUT1 transporters at the BBB explain hypometabolism, which occurs before the onset of cognitive dysfunction and amplifies neurodegenerative processes [73–75]. Such alterations are however also found in other neurodegenerative diseases such as Parkinson's disease [43,76]. Further, increased GLUT1 phosphorylation in major depressive disorder was alleviated in patients who remitted after treatment [77]. Thus, BBB transfer by GLUT1 may represent a promising therapeutic target for various disorders to rescue brain glucose metabolism [12,78].

Finally, the herein proposed concepts may at least partly translate to other targets such as dopamine and serotonin synthesis, imaged with 6-[$^{18}$F]FDOPA [79] and [$^{11}$C]AMT [80], respectively, as numerous of the presented aspects apply in a similar manner. These include facilitated transport across the BBB (via the L-type amino acid transporter 1 [81,82]), a low extraction rate from blood [83] and a tight coupling of BBB transport [84] and neurotransmitter synthesis enzymes [85–88] with neuronal activation. Future application of this approach may therefore provide novel insights into neurotransmitter dysfunction in psychiatric disorders.

**Supplementary Materials:** The following supporting information can be downloaded at the website of this paper posted on Preprints.org.

**Acknowledgements:** We thank the graduated team members and the diploma students of the Neuroimaging Lab (NIL, head: R. Lanzenberger) as well as the clinical colleagues from the Department of Psychiatry and Psychotherapy for clinical and/or administrative support. In detail, we would like to thank L. Silberbauer, and G. Gryglewski for medical support, L. Rischka for acquisition and analysis support. The scientific project was performed with the support of the Medical Imaging Cluster of the Medical University of Vienna.

**Funding:** This research was funded in whole or in part by the Austrian Science Fund (FWF) [Grant DOI 10.55776/KLI610 and 10.55776/KLI1151, PI: A. Hahn, Grant DOI 10.55776/KLI1006, PI: R. Lanzenberger]. For the purpose of open access, the author has applied a CC BY public copyright license to any Author Accepted Manuscript version arising from this submission. C. Milz is a recipient of a DOC Fellowship (27221) from the Austrian Academy of Sciences at the Department of Psychiatry and Psychotherapy, Medical University of Vienna.

**Author Contributions:** Conceptualization: A.H., R.L. Methodology: P.F., A.H. Writing – original draft: A.H., M.M., P.F. Writing – review and editing: all authors. Funding acquisition: A.H., R.L., C.M. All authors discussed the implications, revised the manuscript and approved the final version.

**Conflict of Interest:** RL received investigator-initiated research funding from Siemens Healthcare regarding clinical research using PET/MR. He is a shareholder of the start-up company BM Health GmbH since 2019. M. Hacker received consulting fees and/or honoraria from Bayer Healthcare BMS, Eli Lilly, EZAG, GE Healthcare, Ipsen, ITM, Janssen, Roche, and Siemens Healthineers. All other authors report no conflict of interest in relation to this study.

**Data and Code Availability:** Custom code for simulations can be obtained from the corresponding author with a transfer agreement.

 doi:10.20944/preprints202502.0892.v1



## References


1. Wadsak W, Mitterhauser M. Basics and principles of radiopharmaceuticals for PET/CT. *Eur J Radiol.* Mar 2010;73(3):461-469.
2. Buerkle A, Weber WA. Imaging of tumor glucose utilization with positron emission tomography. *Cancer and Metastasis Reviews.* 2008-12-01 2008;27(4):545-554.
3. Guedj E, Varrone A, Boellaard R, et al. EANM procedure guidelines for brain PET imaging using [(18)F]FDG, version 3. *Eur J Nucl Med Mol Imaging.* Jan 2022;49(2):632-651.
4. Villien M, Wey HY, Mandeville JB, et al. Dynamic functional imaging of brain glucose utilization using fPET-FDG. *Neuroimage.* Oct 15 2014;100:192-199.
5. Hahn A, Gryglewski G, Nics L, et al. Quantification of Task-Specific Glucose Metabolism with Constant Infusion of 18F-FDG. *J Nucl Med.* Dec 2016;57(12):1933-1940.
6. Jamadar SD, Ward PG, Li S, et al. Simultaneous task-based BOLD-fMRI and [18-F] FDG functional PET for measurement of neuronal metabolism in the human visual cortex. *Neuroimage.* Apr 1 2019;189:258-266.
7. Rischka L, Gryglewski G, Pfaff S, et al. Reduced task durations in functional PET imaging with [(18)F]FDG approaching that of functional MRI. *Neuroimage.* Jun 30 2018;181:323-330.
8. Hahn A, Reed MB, Vraka C, et al. High-temporal resolution functional PET/MRI reveals coupling between human metabolic and hemodynamic brain response. *Eur J Nucl Med Mol Imaging.* Dec 6 2023.
9. Dienel GA. Brain Glucose Metabolism: Integration of Energetics with Function. *Physiol Rev.* Jan 1 2019;99(1):949-1045.
10. Jamadar S, Behler A, Deery H, Breakspear PM. The metabolic costs of cognition. 2024-07-22 2024.
11. Simpson IA, Carruthers A, Vannucci SJ. Supply and Demand in Cerebral Energy Metabolism: The Role of Nutrient Transporters. *Journal of Cerebral Blood Flow & Metabolism.* 2007-11-01 2007;27(11):1766-1791.
12. Patching SG. Glucose Transporters at the Blood-Brain Barrier: Function, Regulation and Gateways for Drug Delivery. *Molecular Neurobiology.* 2017-03-01 2017;54(2):1046-1077.
13. Koepsell H. Glucose transporters in brain in health and disease. *Pflügers Archiv - European Journal of Physiology.* 2020-09-01 2020;472(9):1299-1343.
14. Leybaert L. Neurobarrier coupling in the brain: a partner of neurovascular and neurometabolic coupling? *J Cereb Blood Flow Metab.* Jan 2005;25(1):2-16.
15. Rothman DL, Dienel GA, Behar KL, et al. Glucose sparing by glycogenolysis (GSG) determines the relationship between brain metabolism and neurotransmission. *J Cereb Blood Flow Metab.* May 2022;42(5):844-860.
16. Barros LF, Porras OH, Bittner CX. Why glucose transport in the brain matters for PET. *Trends in Neurosciences.* 2005-03-01 2005;28(3):117-119.
17. Leybaert L, De Bock M, Van Moorhem M, Decrock E, De Vuyst E. Neurobarrier coupling in the brain: Adjusting glucose entry with demand. *Journal of Neuroscience Research.* 2007 2007;85(15):3213-3220.
18. Barros LF, Bittner CX, Loaiza A, Porras OH. A quantitative overview of glucose dynamics in the gliovascular unit. *Glia.* Sep 2007;55(12):1222-1237.
19. Furler SM, Jenkins AB, Storlien LH, Kraegen EW. In vivo location of the rate-limiting step of hexose uptake in muscle and brain tissue of rats. *Am J Physiol.* Sep 1991;261(3 Pt 1):E337-347.
20. Robinson PJ, Rapoport SI. Glucose transport and metabolism in the brain. *Am J Physiol.* Jan 1986;250(1 Pt 2):R127-136.
21. Gruetter R, Novotny EJ, Boulware SD, Rothman DL, Shulman RG. 1H NMR studies of glucose transport in the human brain. *J Cereb Blood Flow Metab.* May 1996;16(3):427-438.
22. Dienel GA, Cruz NF. Contributions of glycogen to astrocytic energetics during brain activation. *Metabolic Brain Disease.* 2015-02-01 2015;30(1):281-298.
23. Tomlinson DR, Gardiner NJ. Glucose neurotoxicity. *Nature Reviews Neuroscience.* 2008-01 2008;9(1):36-45.
24. Godbersen GM, Falb P, Klug S, et al. Non-invasive assessment of stimulation-specific changes in cerebral glucose metabolism with functional PET. *Eur J Nucl Med Mol Imaging.* Jul 2024;51(8):2283-2292.
25. Hu Y, Wilson GS. Rapid Changes in Local Extracellular Rat Brain Glucose Observed with an In Vivo Glucose Sensor. *Journal of Neurochemistry.* 1997 1997;68(4):1745-1752.

 doi:10.20944/preprints202502.0892.v1




26. Chen W, Novotny EJ, Zhu XH, Rothman DL, Shulman RG. Localized 1H NMR measurement of glucose consumption in the human brain during visual stimulation. *Proc Natl Acad Sci U S A.* Nov 1 1993;90(21):9896-9900.
27. Fox PT, Raichle ME, Mintun MA, Dence C. Nonoxidative glucose consumption during focal physiologic neural activity. *Science.* Jul 22 1988;241(4864):462-464.
28. Fang J, Ohba H, Hashimoto F, Tsukada H, Chen F, Liu H. Imaging mitochondrial complex I activation during a vibrotactile stimulation: A PET study using [(18)F]BCPP-EF in the conscious monkey brain. *J Cereb Blood Flow Metab.* Dec 2020;40(12):2521-2532.
29. Kessler RM. Imaging methods for evaluating brain function in man. *Neurobiol Aging.* May-Jun 2003;24 Suppl 1:S21-35; discussion S37-29.
30. Mintun MA, Lundstrom BN, Snyder AZ, Vlassenko AG, Shulman GL, Raichle ME. Blood flow and oxygen delivery to human brain during functional activity: theoretical modeling and experimental data. *Proc Natl Acad Sci U S A.* Jun 5 2001;98(12):6859-6864.
31. Fox PT, Raichle ME. Focal physiological uncoupling of cerebral blood flow and oxidative metabolism during somatosensory stimulation in human subjects. *Proc Natl Acad Sci U S A.* Feb 1986;83(4):1140-1144.
32. Li B, Freeman RD. Neurometabolic coupling between neural activity, glucose, and lactate in activated visual cortex. *J Neurochem.* Nov 2015;135(4):742-754.
33. Roche R, Salazar P, Martin M, Marcano F, Gonzalez-Mora JL. Simultaneous measurements of glucose, oxyhemoglobin and deoxyhemoglobin in exposed rat cortex. *J Neurosci Methods.* Nov 15 2011;202(2):192-198.
34. Mann K, Deny S, Ganguli S, Clandinin TR. Coupling of activity, metabolism and behaviour across the Drosophila brain. *Nature.* May 2021;593(7858):244-248.
35. Hawkins RA, Mans AM, Davis DW, Hibbard LS, Lu DM. Glucose availability to individual cerebral structures is correlated to glucose metabolism. *J Neurochem.* Apr 1983;40(4):1013-1018.
36. Hargreaves RJ, Planas AM, Cremer JE, Cunningham VJ. Studies on the relationship between cerebral glucose transport and phosphorylation using 2-deoxyglucose. *J Cereb Blood Flow Metab.* Dec 1986;6(6):708-716.
37. Phelps ME, Kuhl DE, Mazziota JC. Metabolic mapping of the brain's response to visual stimulation: studies in humans. *Science.* Mar 27 1981;211(4489):1445-1448.
38. Vlassenko AG, Rundle MM, Mintun MA. Human brain glucose metabolism may evolve during activation: findings from a modified FDG PET paradigm. *Neuroimage.* Dec 2006;33(4):1036-1041.
39. Mishra A, Reynolds JP, Chen Y, Gourine AV, Rusakov DA, Attwell D. Astrocytes mediate neurovascular signaling to capillary pericytes but not to arterioles. *Nat Neurosci.* Dec 2016;19(12):1619-1627.
40. Kleinfeld D, Mitra PP, Helmchen F, Denk W. Fluctuations and stimulus-induced changes in blood flow observed in individual capillaries in layers 2 through 4 of rat neocortex. *Proceedings of the National Academy of Sciences.* 1998-12-22 1998;95(26):15741-15746.
41. Vogel J, Kuschinsky W. Decreased Heterogeneity of Capillary Plasma Flow in the Rat Whisker-Barrel Cortex during Functional Hyperemia. *Journal of Cerebral Blood Flow & Metabolism.* 1996-11-01 1996;16(6):1300-1306.
42. Akgören N, Lauritzen M. Functional recruitment of red blood cells to rat brain microcirculation accompanying increased neuronal activity in cerebellar cortex. *NeuroReport.* November 8, 1999 1999;10(16):3257.
43. Barros LF, San Martín A, Ruminot I, et al. Near-critical GLUT1 and Neurodegeneration. *Journal of Neuroscience Research.* 2017 2017;95(11):2267-2274.
44. Hasselbalch SG, Holm S, Pedersen HS, et al. The (18)F-fluorodeoxyglucose lumped constant determined in human brain from extraction fractions of (18)F-fluorodeoxyglucose and glucose. *J Cereb Blood Flow Metab.* Aug 2001;21(8):995-1002.
45. Fellows LK, Boutelle MG, Fillenz M. Extracellular brain glucose levels reflect local neuronal activity: a microdialysis study in awake, freely moving rats. *J Neurochem.* Dec 1992;59(6):2141-2147.
46. McNay EC, Fries TM, Gold PE. Decreases in rat extracellular hippocampal glucose concentration associated with cognitive demand during a spatial task. *Proc Natl Acad Sci U S A.* Mar 14 2000;97(6):2881-2885.

 doi:10.20944/preprints202502.0892.v1




47. Barnes K, Ingram JC, Bennett MDM, Stewart GW, Baldwin SA. Methyl-beta-cyclodextrin stimulates glucose uptake in Clone 9 cells: a possible role for lipid rafts. *Biochem J.* 2004-03-01 2004;378(2):343-351.
48. Caliceti C, Zambonin L, Prata C, et al. Effect of plasma membrane cholesterol depletion on glucose transport regulation in leukemia cells. *PLoS One.* 2012;7(7):e41246.
49. Park M-S. Molecular Dynamics Simulations of the Human Glucose Transporter GLUT1. *PLOS ONE.* 28.04.2015 2015;10(4):e0125361.
50. Mitrovic D, McComas SE, Alleva C, Bonaccorsi M, Drew D, Delemotte L. Reconstructing the transport cycle in the sugar porter superfamily using coevolution-powered machine learning. *eLife.* 2023-07-05 2023;12:e84805.
51. Hamrahian AH, Zhang J-Z, Elkhairi FS, Prasad R, Ismail-Beigi F. Activation of Glut1 Glucose Transporter in Response to Inhibition of Oxidative Phosphorylation: Role of Sites of Mitochondrial Inhibition and Mechanism of Glut1 Activation. *Archives of Biochemistry and Biophysics.* 1999-08-15 1999;368(2):375-379.
52. Barnes K, Ingram JC, Porras OH, et al. Activation of GLUT1 by metabolic and osmotic stress: potential involvement of AMP-activated protein kinase (AMPK). *Journal of Cell Science.* 2002-06-01 2002;115(11):2433-2442.
53. Mercado CL, Loeb JN, Ismail-Beigi F. Enhanced glucose transport in response to inhibition of respiration in Clone 9 cells. *American Journal of Physiology-Cell Physiology.* 1989-07 1989;257(1):C19-C28.
54. Yan Q, Lu Y, Zhou L, et al. Mechanistic insights into GLUT1 activation and clustering revealed by super-resolution imaging. *Proceedings of the National Academy of Sciences.* 2018-07-03 2018;115(27):7033-7038.
55. Loaiza A, Porras OH, Barros LF. Glutamate Triggers Rapid Glucose Transport Stimulation in Astrocytes as Evidenced by Real-Time Confocal Microscopy. *Journal of Neuroscience.* 2003/08/13 2003;23(19):7337-7342.
56. Cornford EM, Nguyen EV, Landaw EM. Acute upregulation of blood-brain barrier glucose transporter activity in seizures. *American Journal of Physiology-Heart and Circulatory Physiology.* 2000-09 2000;279(3):H1346-H1354.
57. Shetty M, Loeb JN, Vikstrom K, Ismail-Beigi F. Rapid activation of GLUT-1 glucose transporter following inhibition of oxidative phosphorylation in clone 9 cells. *Journal of Biological Chemistry.* 1993-08-01 1993;268(23):17225-17232.
58. Biswal B, Yetkin FZ, Haughton VM, Hyde JS. Functional connectivity in the motor cortex of resting human brain using echo-planar MRI. *Magn Reson Med.* 1995;34(4):537-541.
59. Fox MD, Snyder AZ, Vincent JL, Corbetta M, Van Essen DC, Raichle ME. The human brain is intrinsically organized into dynamic, anticorrelated functional networks. *Proc Natl Acad Sci U S A.* 2005;102(27):9673-9678.
60. Fox MD, Raichle ME. Spontaneous fluctuations in brain activity observed with functional magnetic resonance imaging. *Nature Reviews. Neuroscience.* 2007;8(9):700-711.
61. Margulies DS, Ghosh SS, Goulas A, et al. Situating the default-mode network along a principal gradient of macroscale cortical organization. *Proc Natl Acad Sci U S A.* Nov 1 2016;113(44):12574-12579.
62. Smith SM, Fox PT, Miller KL, et al. Correspondence of the brain's functional architecture during activation and rest. *Proc Natl Acad Sci U S A.* Aug 4 2009;106(31):13040-13045.
63. Horwitz B, Duara R, Rapoport SI. Intercorrelations of glucose metabolic rates between brain regions: application to healthy males in a state of reduced sensory input. *J Cereb Blood Flow Metab.* Dec 1984;4(4):484-499.
64. McIntosh AR, Grady CL, Ungerleider LG, Haxby JV, Rapoport SI, Horwitz B. Network analysis of cortical visual pathways mapped with PET. *J Neurosci.* Feb 1994;14(2):655-666.
65. Reed M, Cocchi L, Knudsen G, et al. Connecting the Dots: Approaching a Standardized Nomenclature for Molecular Connectivity Combining Data and Literature. *bioRxiv.* 2024:2024.2005.2010.593490.
66. Jamadar SD, Ward PGD, Liang EX, Orchard ER, Chen Z, Egan GF. Metabolic and Hemodynamic Resting-State Connectivity of the Human Brain: A High-Temporal Resolution Simultaneous BOLD-fMRI and FDG-fPET Multimodality Study. *Cereb Cortex.* May 10 2021;31(6):2855-2867.
67. Sala A, Lizarraga A, Caminiti SP, et al. Brain connectomics: time for a molecular imaging perspective? *Trends Cogn Sci.* Apr 2023;27(4):353-366.

 doi:10.20944/preprints202502.0892.v1




68. Hahn A, Reed MB, Milz C, Falb P, Murgaš M, Lanzenberger R. A Unified Approach for Identifying PET-based Neuronal Activation and Molecular Connectivity with the functional PET toolbox. *BioRxiv.* 2024.
69. Reed MB, Ponce de Leon M, Vraka C, et al. Whole-body metabolic connectivity framework with functional PET. *Neuroimage.* May 1 2023;271:120030.
70. Raichle ME. The restless brain. *Brain Connect.* 2011;1(1):3-12.
71. Hu Y, Wilson GS. A Temporary Local Energy Pool Coupled to Neuronal Activity: Fluctuations of Extracellular Lactate Levels in Rat Brain Monitored with Rapid-Response Enzyme-Based Sensor. *Journal of Neurochemistry.* 1997 1997;69(4):1484-1490.
72. Dienel GA. Lack of appropriate stoichiometry: Strong evidence against an energetically important astrocyte–neuron lactate shuttle in brain. *Journal of Neuroscience Research.* 2017 2017;95(11):2103-2125.
73. Winkler EA, Nishida Y, Sagare AP, et al. GLUT1 reductions exacerbate Alzheimer's disease vasculo-neuronal dysfunction and degeneration. *Nature Neuroscience.* 2015-04 2015;18(4):521-530.
74. Erickson MA, Banks WA. Blood–Brain Barrier Dysfunction as a Cause and Consequence of Alzheimer's Disease. *Journal of Cerebral Blood Flow & Metabolism.* 2013-10-01 2013;33(10):1500-1513.
75. Szablewski L. Glucose Transporters in Brain: In Health and in Alzheimer's Disease. *Journal of Alzheimer's Disease.* 2017-01-01 2017;55(4):1307-1320.
76. Zhang S, Lachance BB, Mattson MP, Jia X. Glucose metabolic crosstalk and regulation in brain function and diseases. *Progress in Neurobiology.* 2021-09-01 2021;204:102089.
77. Kahl KG, Georgi K, Bleich S, et al. Altered DNA methylation of glucose transporter 1 and glucose transporter 4 in patients with major depressive disorder. *Journal of Psychiatric Research.* 2016-05-01 2016;76:66-73.
78. Cunnane SC, Trushina E, Morland C, et al. Brain energy rescue: an emerging therapeutic concept for neurodegenerative disorders of ageing. *Nature Reviews Drug Discovery.* 2020-09 2020;19(9):609-633.
79. Hahn A, Reed MB, Pichler V, et al. Functional dynamics of dopamine synthesis during monetary reward and punishment processing. *J Cereb Blood Flow Metab.* 2021;41(11):2973-2985.
80. Hahn A, Reed MB, Murgas M, et al. Dynamics of human serotonin synthesis differentially link to reward anticipation and feedback. *Mol Psychiatry.* Aug 23 2024.
81. del Amo EM, Urtti A, Yliperttula M. Pharmacokinetic role of L-type amino acid transporters LAT1 and LAT2. *Eur J Pharm Sci.* Oct 2 2008;35(3):161-174.
82. Zaragoza R. Transport of Amino Acids Across the Blood-Brain Barrier. *Frontiers in physiology.* 2020;11:973.
83. Muzik O, Chugani DC, Chakraborty P, Mangner T, Chugani HT. Analysis of [C-11]alpha-methyl-tryptophan kinetics for the estimation of serotonin synthesis rate in vivo. *J Cereb Blood Flow Metab.* Jun 1997;17(6):659-669.
84. Delescluse J, Simonnet MM, Ziegler AB, et al. A LAT1-Like Amino Acid Transporter Regulates Neuronal Activity in the Drosophila Mushroom Bodies. *Cells.* Aug 13 2024;13(16).
85. Hery F, Simonnet G, Bourgoin S, et al. Effect of nerve activity on the in vivo release of [3H]serotonin continuously formed from L-[3H]tryptophan in the caudate nucleus of the cat. *Brain Res.* Jun 22 1979;169(2):317-334.
86. Hamon M, Bourgoin S, Artaud F, Glowinski J. The role of intraneuronal 5-HT and of tryptophan hydroxylase activation in the control of 5-HT synthesis in rat brain slices incubated in K+-enriched medium. *J Neurochem.* Nov 1979;33(5):1031-1042.
87. Morgenroth VH, 3rd, Boadle-Biber M, Roth RH. Tyrosine hydroxylase: activation by nerve stimulation. *Proc Natl Acad Sci U S A.* Nov 1974;71(11):4283-4287.
88. Neff NH, Hadjiconstantinou M. Aromatic L-amino acid decarboxylase modulation and Parkinson's disease. *Prog Brain Res.* 1995;106:91-97.
89. Silberbauer L, Reed M, Murgas M, et al. Assessment of cerebral glucose metabolism and blood flow following acute citalopram challenge. *Neuroscience Applied.* 2022/01/01/ 2022;1:100682.
90. Duarte JM, Gruetter R. Characterization of cerebral glucose dynamics in vivo with a four-state conformational model of transport at the blood-brain barrier. *J Neurochem.* May 2012;121(3):396-406.

 doi:10.20944/preprints202502.0892.v1



91. Gruetter R, Ugurbil K, Seaquist ER. Steady-state cerebral glucose concentrations and transport in the human brain. *J Neurochem.* Jan 1998;70(1):397-408.
92. Cunningham VJ, Hargreaves RJ, Pelling D, Moorhouse SR. Regional blood-brain glucose transfer in the rat: a novel double-membrane kinetic analysis. *J Cereb Blood Flow Metab.* Jun 1986;6(3):305-314.